

A Study on Improvement of Lift-Drag Characteristics of Transonic Airfoil with Passive Ventilation

Tani, Yasuhiro
Fuji Heavy Industries Co. Ltd. : Senior Engineer

Aso, Shigeru
Department of Aeronautics and Astronautics : Professor

<https://hdl.handle.net/2324/3322>

出版情報 : 九州大学工学紀要. 64 (1), pp.101-110, 2004-03. 九州大学大学院工学研究院
バージョン :
権利関係 :



A Study on Improvement of Lift-Drag Characteristics of Transonic Airfoil with Passive Ventilation

by

Yasuhiro TANI* and Shigeru ASO**

(Received January 5, 2004)

Abstract

An experimental and computational study on improvement of lift-drag characteristics of transonic airfoil with passive ventilation has been conducted. Transonic airfoils with passive ventilation have been selected in the present study. For the passive ventilation, porous wall on the upper surface of wing or a pair of slits, which are located on the wing surface, is used. Surface pressure distributions on the airfoil are measured in order to investigate the effect of passive ventilation to the improvement of lift-drag characteristics of the airfoil. Lift and drag coefficients of the airfoil are calculated by using those surface pressure distributions. The results show the passive ventilation could improve lift-drag characteristics of the airfoil in some cases and the optimal selections of the shape of airfoil and location of passive ventilation are requested.

Keywords: Supercritical wing, Passive ventilation, Wing, Transonic flow, Lift-drag characteristics

1. Introduction

For the transonic transports, drag reduction and high speed performance are the most required problem. The shock wave appears on the airfoil at transonic regime and the shock-boundary layer interaction is inevitable. To relieve this interaction, some types of ventilation mechanism have been proposed.^{1)~6)}

Ventilation mechanisms are classified into two groups, one is an active ventilation mechanism with external supplied power, and the other one is the passive ventilation. Passive ventilation mechanism has a pair of slits connected each other by an internal channel or porous surface with a cavity underneath it. Ventilation flow is driven by the surface pressure difference between the slits or porous region. Some experimental and numerical results have been reported that the passive ventilation with porous or slits located around the shock wave can bring drag reduction and Mdd improvement at transonic speed regime.

* Senior Engineer, Fuji Heavy Industries, Co. Ltd.

** Professor, Department of Aeronautics and Astronautics

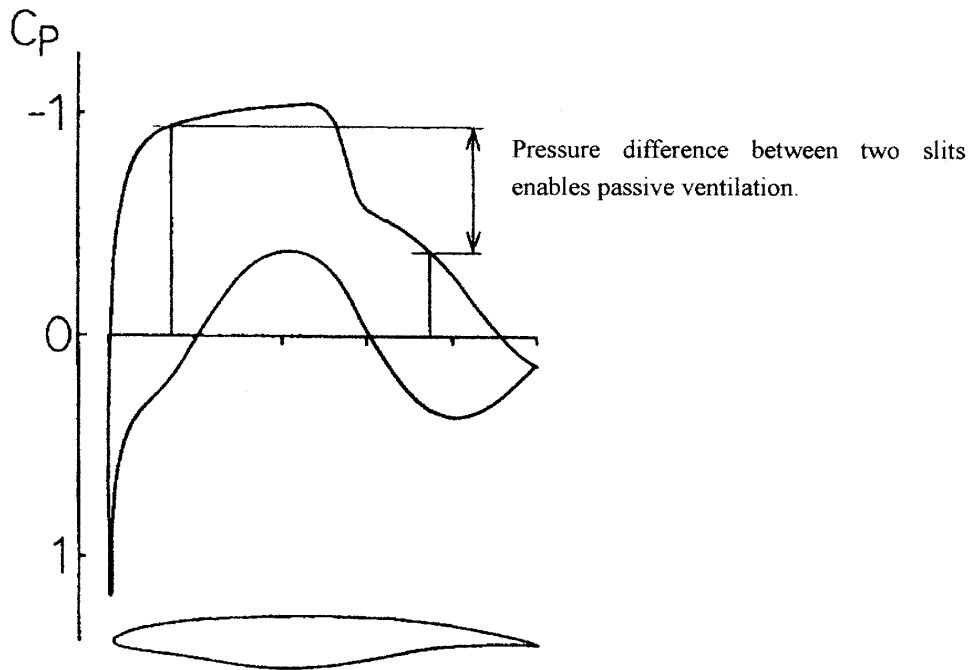


Fig. 1 Schematic sketch of the new concept of passive ventilation with slits.

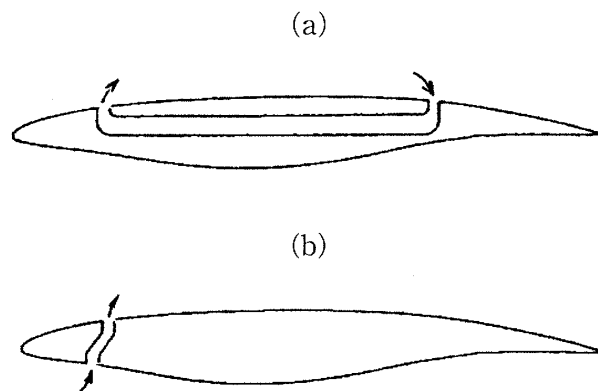


Fig. 2 Two types of the new concept of passive ventilation with slits.
 (a) Ventilation Type-1
 (b) Ventilation Type-2

In this paper, in addition to the porous wall, a new concept of passive ventilation by slits is applied on transonic airfoils. **Figure 1** shows the schematic sketch of this concept. Pressure difference between the slits derives the ventilation flow; blowing and suction at the slits and internal flow in a duct. Blowing from the slit at the lower pressure region near the leading edge of the airfoil, and suction into the slit at higher pressure region near the trailing edge. The blowing flow speed is slower than the outer flow around the airfoil, so the slower flow layer is formed on the airfoil surface downstream of the blowing slit. It is expected that the frictional drag reduce in this region. Furthermore the larger displacement thickness of the boundary layer is formed, which is equivalent to the additional airfoil camber line, so it brings more lift. This slower flow on the airfoil surface is sucked into the slit near the trailing edge and it enables good pressure recovery at the trailing edge. Consequently, the reduction of both frictional and pressure drag are expected by this concept of ventilation. In

this study, two types of passive ventilation with slits are proposed, shown in **Fig. 2**.

2. Experiments and Numerical Methods

To investigate the effect of the passive ventilation, an experimental and computational study was conducted. Transonic wind tunnel tests and Navier-Stokes computations were carried out on transonic airfoils with passive ventilation.

2.1 Experimental Models and Facilities

One of the experimental investigations in this study was carried out in the 61cm Fuji Heavy Industries (FHI) trisonic wind tunnel.^{7,8,9)} The model tested was a two-dimensional supercritical airfoil A-10, which has both front and rear loading shape and 12% thickness ratio. The chord length of the model is 200mm and its span is the wind tunnel width. Interchangeable inserts were equipped on the upper surface of the airfoil, one is a porous surface, 0.1mm of diameter and 1.0mm pitch, on the mid-chord region and the other is a pair of slits at 15%C and 75%C location, whose width is 1mm in chord wise. Surface pressure distribution was measured at 48 positions in the mid-span plane. The lift was obtained by integrating the surface pressure distributions, and the drag from total pressure measurements by the wake rake. Boundary layer trip strips were placed near the leading edge on both sides.

Another experimental investigation was carried out at the NAE trisonic wind tunnel in Canada with two-dimensional test section for higher Reynolds number conditions.⁹⁾ The model used in this test was 304.8mm chord length and 381mm span width two-dimensional supercritical airfoil UVA-1 model. Slits were located at 12%C and 70%C on the upper surface and 12%C on the lower surface on the interchangeable inserts. The lift was obtained by integrating the pressure distribution measured at 68 points on the surface, and drag from total pressure measurements by the wake rake.

2.2 Numerical Procedure

In Addition to the wind tunnel test, numerical investigations were carried out to analyze detail phenomena of the ventilation effect.¹⁰⁾ Two-dimensional unsteady compressible thin-layer Navier-Stokes equations were adopted in this study. The numerical procedure to solve the governing equations is a modified form of the LU-ADI scheme.¹¹⁾ Chakravarty-Osher's upwind difference¹²⁾ and space variable time step method have been incorporated. An algebraic turbulence model developed by Baldwin and Lomax was used to calculate eddy viscosity.¹³⁾

To simulate the effect of the ventilation numerically, an improved boundary condition was applied to the slit and porous region on the airfoil. This is an extension of that for porous surface used by Chen et al.^{4,5)} and is based on Darcy's Law for the perforated media.

Velocity normal to the surface through the slit is governed such that

$$V_n = -(1/2)\sigma(C_P - \overline{C_P})$$

$$\sigma = \overline{\sigma} U_\infty / a^*$$

C_P and $\overline{C_P}$ are the pressure coefficients above and below the slit surface respectively. Flow velocity is expected to be slower than outer flow, so that $\overline{C_P}$ is assumed to be constant in the cavity. $\overline{\sigma}$ is the porosity distribution function, which was determined by the wind tunnel test results of channel mass flow. a^* is the critical sound speed, and U_∞ is the uniform velocity. The mass flow through the slits must be zero,

$$Q = \int_s \rho V_n ds = 0$$

which gives, by assuming constant channel pressure,

$$\overline{C_P} = \int_s \sigma \rho C_P ds / \int_s \sigma \rho ds$$

C_P , the pressure coefficient at the slit surface, is calculated from the momentum equation of the normal direction to the surface.

3. The Effect of Passive Ventilation

Experimental and numerical results on passive ventilation are checked by the following points; pressure distribution, boundary layer profile, special flow pattern around the airfoil, and lift-drag characteristics.

3.1 Pressure Distribution

Figure 3 shows the surface pressure distributions for ventilation with porous surface at transonic speed. Pressure distribution on the porous surface becomes flat and the single strong shock wave was divided into two weak ones.

Figure 4 shows the wind tunnel test results for the ventilation with slits. Comparison of surface pressure distribution at $M=0.60$ and $M=0.75$ between No-Ventilation and Ventilation Type-1 configuration is shown. Slower blowing from the slit near the leading edge by the ventilation causes thicker displacement thickness of the boundary layer, and it is equivalent to change of the camber line of the airfoil. So it decreases surface pressure between the slits.

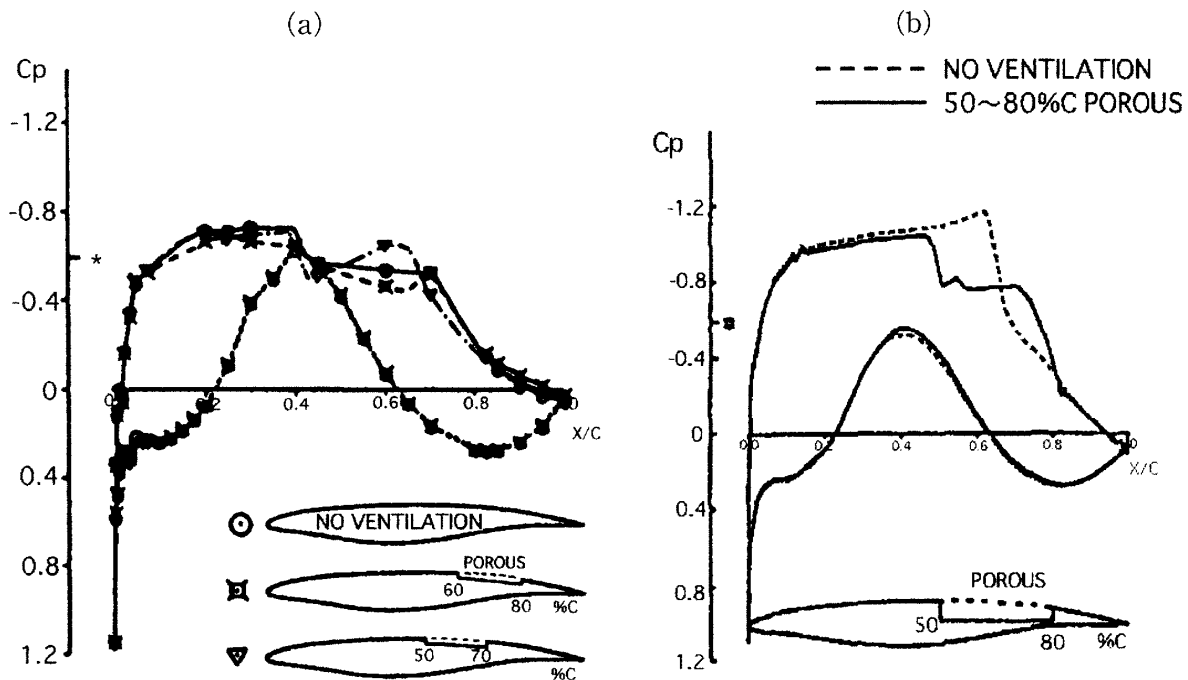


Fig. 3 Comparison of surface pressure distribution; Ventilation with porous surface and No-Ventilation (A-10 airfoil, wind tunnel test).
 (a) Wind tunnel test result
 (b) NS computation result

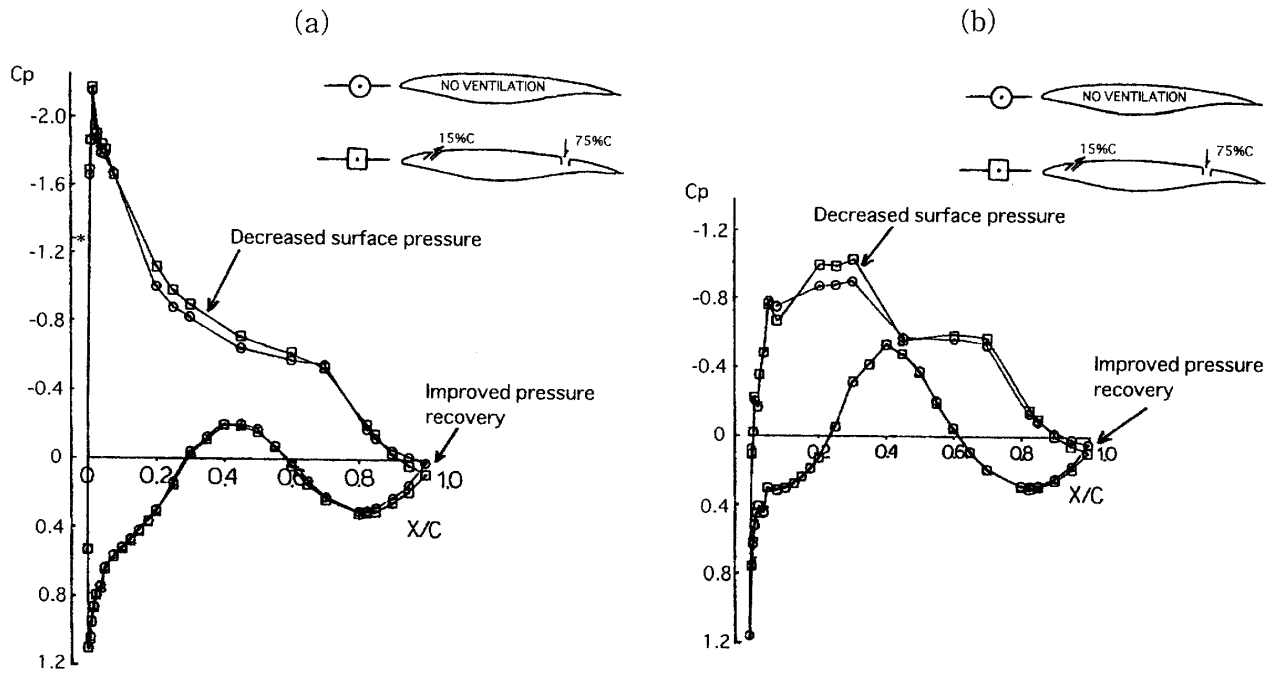


Fig. 4 Comparison of surface pressure distribution; Ventilation Type-1 and No-Ventilation (A-10 airfoil, wind tunnel test result).

(a) $M=0.6$, $\alpha=2.0^\circ$, $Re=2.2 \times 10^6$
 (b) $M=0.75$, $\alpha=2.0^\circ$, $Re=2.6 \times 10^6$

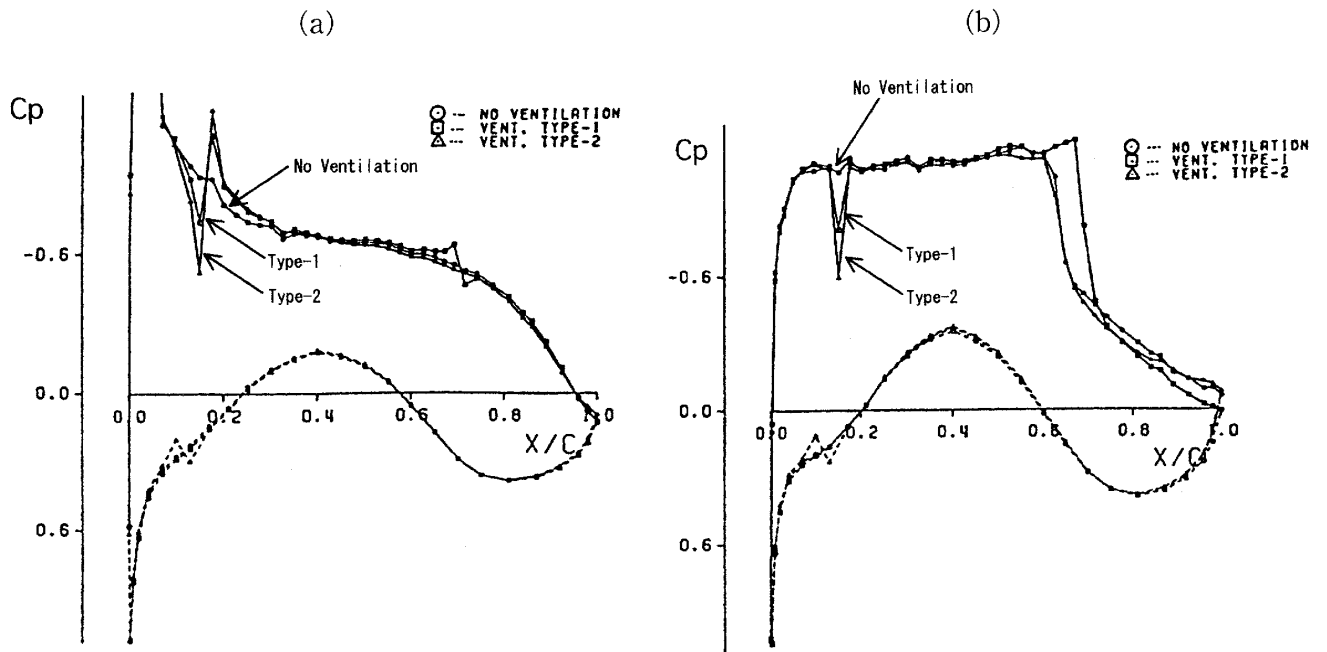


Fig. 5 Comparison of surface pressure distribution; Ventilation Type-1, Type-2 and No-Ventilation (UVA-1 airfoil, wind tunnel test).

(a) $M=0.6$, $\alpha=2.9^\circ$, $Re=14 \times 10^6$
 (b) $M=0.78$, $\alpha=2.7^\circ$, $Re=14 \times 10^6$

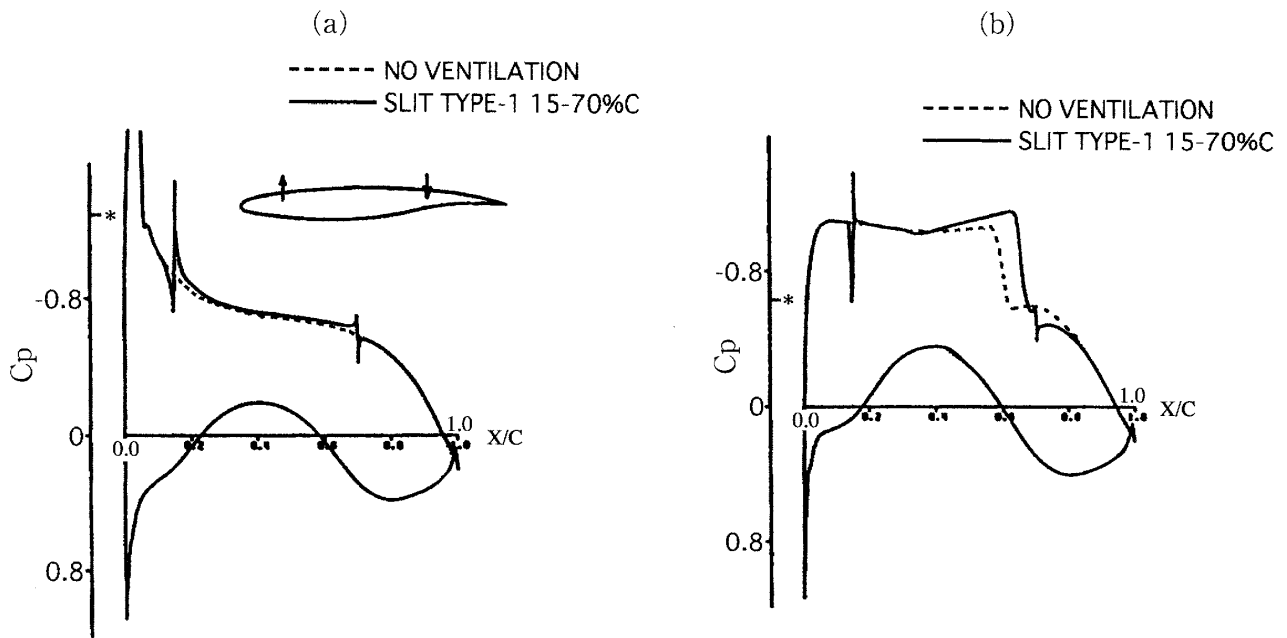


Fig. 6 Comparison of surface pressure distribution; Ventilation Type-1, Type-2 and No-Ventilation (UVA-1 airfoil, NS computation).
 (a) $M=0.6$, $\alpha=3.0^\circ$, $Re=14 \times 10^6$
 (b) $M=0.74$, $\alpha=1.7^\circ$, $Re=14 \times 10^6$

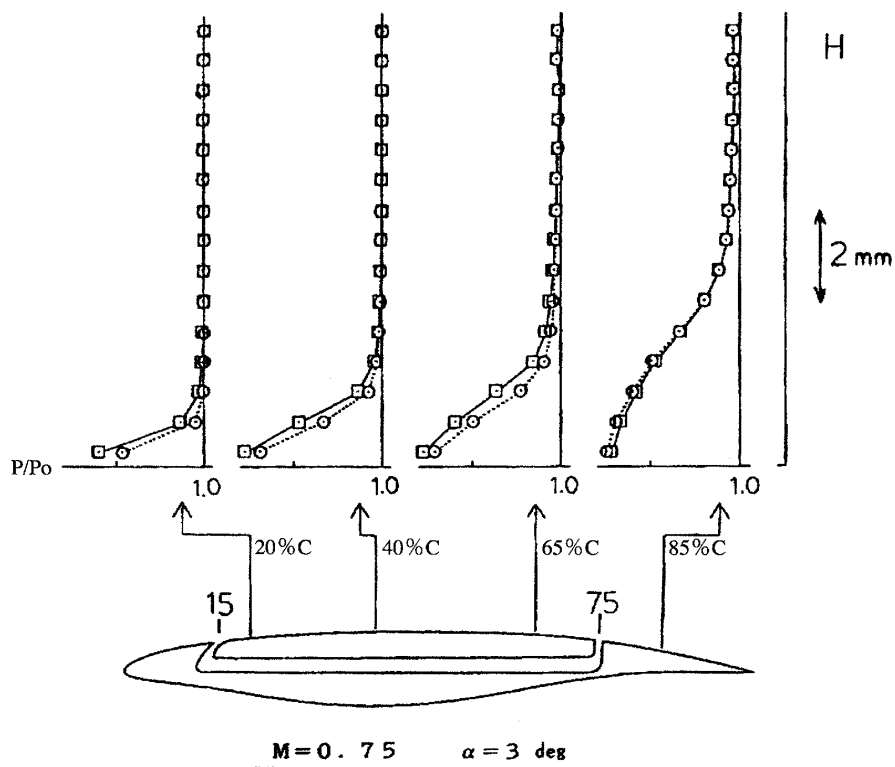


Fig. 7 Comparison of boundary layer profiles; Ventilation Type-1 and No-Ventilation (A-10 airfoil, wind tunnel test).

Figure 5 shows the pressure distributions for UVA-1 airfoil at higher Reynolds number wind tunnel test. The effect of the ventilation is similar to **Fig. 4** for Ventilation Type-1, but the shock wave location moves afterward to the No-Ventilation case. **Figure 6** shows the computation results for the same conditions as wind tunnel test. The result of the ventilation effect shows good agreement to the wind tunnel test results. Peaky compression and expansion is clearly seen around the slit location. For the Ventilation Type-2, so much blowing causes the bigger pressure change around the blowing slit than Ventilation Type-1.

3.2 Boundary Layer Profile

Figure 7 shows the total pressure distributions for the ventilation with slits on the upper surface of the airfoil. It is shown that the slower flow region is formed downstream of the blowing slit at 15%C location. This slower flow region between the slits decreases the skin friction at this region. And this slower flow region is sucked into the slit at 75%C location, so the good pressure recovery can be obtained at the trailing edge.

3.3 Flow Pattern around the Airfoil

Comparison between the isobars by computations of Ventilation Type-1 and No-Ventilation configuration on A-10 airfoil are shown in **Fig. 8** for $M=0.75$. For UVA-1 airfoil, the results of Mach contour on Ventilation Type-1 and Type-2 are shown in **Fig. 9**. As for

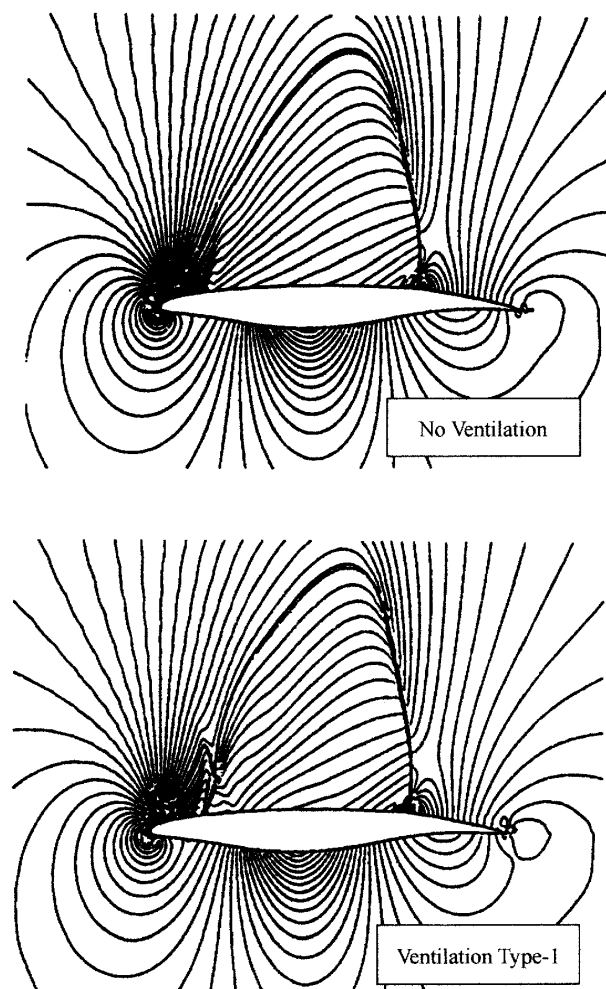


Fig. 8 Comparison of isobars; Ventilation Type-1 and No-Ventilation (A-10 airfoil, NS computation, $M=0.75$, $\alpha=2\text{deg}$).

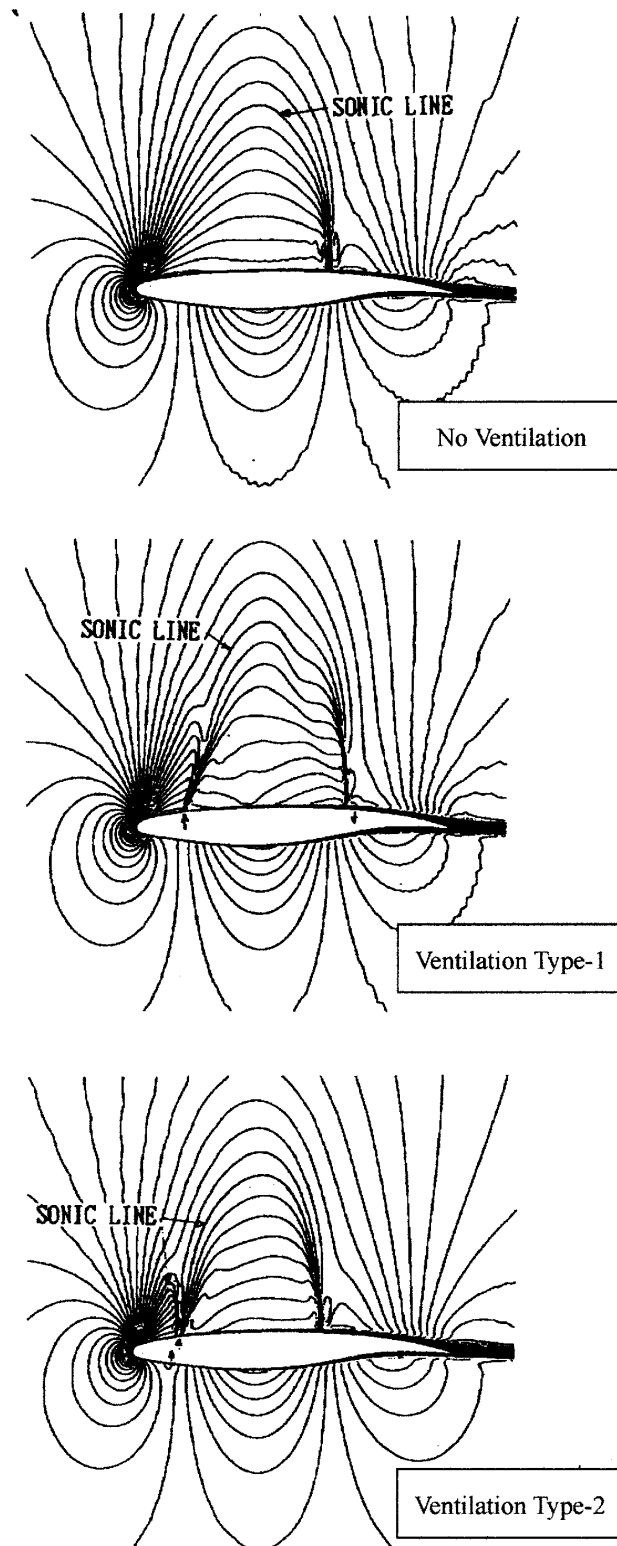


Fig. 9 Comparison of Mach contours; Ventilation Type-1, Type-2 and No-Ventilation (UVA-1 airfoil, NS computation, $M=0.74$, $\alpha=1.7\text{deg}$).

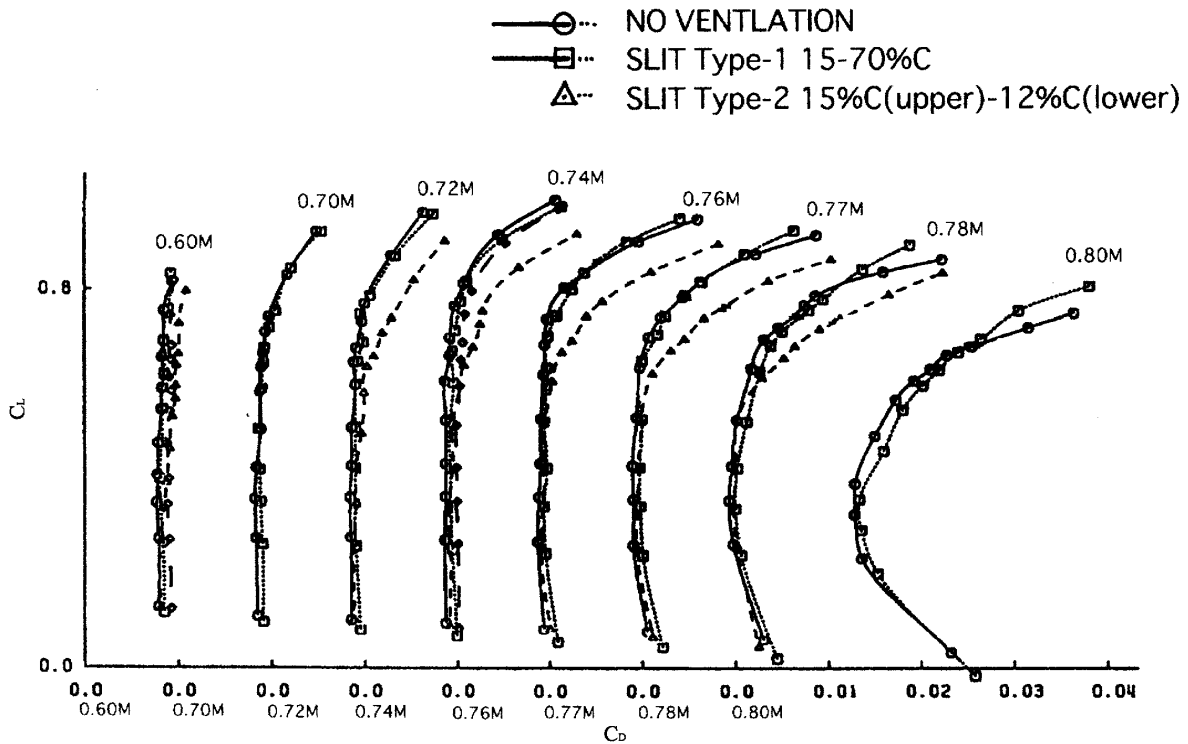


Fig. 10 Comparison of Lift-Drage coefficient; Ventilation Type-1, Type-2 and No-Ventilation (UVA-1 airfoil, wind tunnel test).

Ventilation Type-1, blowing from 15%C slit forms compression and expansion waves in the supersonic region above the airfoil. This compression wave is formed by the increased boundary layer thickness caused by the slower flow blowing, and the expansion wave is formed by the displacement thickness change downstream region of blowing point. These waves propagate in the supersonic region above the airfoil, and reaches to the sonic line. The compression wave reflects as an expansion wave, and it reaches back to the airfoil surface. This causes the decreasing of the surface pressure distribution at this region and increasing of lift coefficient of the airfoil. While the expansion wave generated at the blowing slit reflects as a compression wave at the sonic line, but it seems to be diffused.

For the Ventilation Type-2, blowing from the 15%C slit are stronger than Ventilation Type-1, so the supersonic region above the airfoil are divided into two parts. This causes that there seems to be no wave reflecting phenomena by the ventilation.

3.4 Lift-Drage Characteristics

Figure 10 shows the drag polar for UVA-1 airfoil wind tunnel test. Ventilation Type-1 reduces drag at high Mach number and high angle of attack conditions. However, drag increases slightly at low angle of attack. As for Ventilation Type-2, drag increases at high angle of attack because of the boundary layer separation near the trailing edge caused by too much ventilation blowing flow and the lack of suction.

4. Mechanism of Passive Ventilation

The mechanisms of the new concept of passive ventilation presented in this paper are summarized as follows. Slower flow blowing from the slit forms a slower boundary layer on the airfoil, and it causes the decreasing of the frictional drag at the region between the slits.

This slower flow causes increasing of the airfoil camber, so the lift can be increased. This slower boundary layer flow is sucked into slit near the trailing edge for Type-1, so it does not have bad influence on the pressure recovery at the trailing edge. Further especially for transonic conditions, complicated wave system is formed by the blowing in the supersonic region, and it can decrease surface pressure distribution on the upper surface of the airfoil.

5. Concluding Remarks

An experimental and numerical analysis was carried out on the new concept passive ventilated airfoils with slits. It is shown that the ventilation improves the lift-drag characteristics. This benefit is derived from the frictional drag reduction, lift increment, and suppression of boundary layer separation near the trailing edge. Complicated wave system formed at transonic conditions increases airfoil lift. To achieve an effective passive ventilation, the optimal selection of slit location for the base airfoil is required.

References

- 1) Raghunathan, S., "Passive Control of Shock-Boundary Layer Interaction," *Prog. Aerospace Sci.*, Vol.25, pp.271-296, 1988.
- 2) Krogmann, P. Stanewsky, E., Thiede, P., "Effect of suction on Shock Boundary Layer Interaction and Shock Induced Separation," *J. Aircr.* Vol.22, No.1, Jan. 1985.
- 3) Krogmann, P. and Stanewsky, E., "Transonic Shock-Boundary Layer Interaction Control," ICAS-84-2.3.2, 1984.
- 4) Chen, C. L., Chow, C. Y., Holst, T. L. and Van Dalsem, W. R., "Numerical Simulation of Transonic Flow over Porous Airfoils," AIAA 85-5022, 1985.
- 5) Chen, C. L., Chow, C. Y., Van Dalsem, W. R. and Holst, T. L., "Computation of Viscous Transonic Flow over Porous Airfoils," *J. Aircr.* Vol.26, No.12, Dec. 1989.
- 6) Krenz, G. and Hilbig, R., "Aerodynamic Concepts for Fuel Efficient Transport Aircraft," ICAS-82-1.5.2, 1982.
- 7) Nakadate, M. Koshioka, Y., Kamo, K., Tani, Y., and Amano, K., "Ventilated Airfoils," *Proc. 24th Aircraft Symposium, Tokyo, Japan, Dec. 1988.*
- 8) Koshioka, K., Tani, Y. and Amano, K., "Aerodynamic Characteristics on Ventilated Airfoils," *Proc. 25th Aircraft Symposium, Fukuoka, Japan, Dec. 1989.*
- 9) Tani, Y., Tanaka, K., Amano, K., et.al. "Experimental and Numerical Analysis on Ventilated Airfoils," AIAA 91-3335, 1991.
- 10) Kamo, K., Tani, Y. and Amano, K., "Navier-Stokes Simulation of Transonic Flow Around Ventilated Airfoils," NAL SP-9, pp.133-140, 1988.
- 11) Obayashi, S., Matsushima, K., Fujii, K. and Kuwahawa, K., "Improvements in efficiency and Reliability for Navier-Stokes Computations using LU-ADI Factorization Algorithm," AIAA 85-0338, 1985.
- 12) Chakravarthy, S. R., Osher, S., "A New Class of High Accuracy TVD Schemes for Hyperbolic Conservation Laws," AIAA 85-0363, 1985.
- 13) Baldwin, B. S. and Lomax, H., "Thin Layer Approximation and Algebraic Model for Separated Turbulent Flows," AIAA 78-0257, 1978.